

## Pulsed-Source MOCVD of High- $k$ Dielectric Thin Films with *in situ* Monitoring by Spectroscopic Ellipsometry

Yoshishige TSUCHIYA\*, Masato ENDOH, Masatoshi KUROSAWA<sup>1</sup>, Raymond T. TUNG, Takeo HATTORI<sup>1</sup> and Shunri ODA

Research Center for Quantum Effect Electronics, Tokyo Institute of Technology, 2-12-1, O-okayama, Meguro-ku, Tokyo 152-8552, Japan

<sup>1</sup>Department of Electrical and Electronic Engineering, Musashi Institute of Technology, 1-28-1, Tamazutsumi, Setagaya-ku, Tokyo 158-8557, Japan

(Received October 2, 2002; accepted for publication December 27, 2002)

The formation of high- $k$  thin films by pulsed-source metal-organic chemical vapor deposition (MOCVD) has been investigated with *in situ* spectroscopic ellipsometry. It is demonstrated that spectroscopic ellipsometry is an effective method for *in situ* monitoring of the fabrication of high- $k$  dielectric thin films with thicknesses of several nm's. Thin yttrium oxide films with average roughnesses smaller than the thickness of a single molecular layer, and with a capacitance equivalent thickness  $\sim 1.7$  nm were obtained. Thicknesses and optical properties of each individual layer were also extracted from spectroscopic ellipsometry, by fitting to appropriate structural models. [DOI: 10.1143/JJAP.42.1957]

KEYWORDS: high- $k$  dielectric thin film, pulsed-source MOCVD, *in situ* monitoring of film growth, spectroscopic ellipsometry

### 1. Introduction

The technological requirement in Si-based micro/nano-electronics to overcome the leakage current issue of ultra-thin gate SiO<sub>2</sub> accelerates the search for alternative materials with high dielectric constant (high- $k$ ). For applications in advanced nanoscale Si-devices, these high- $k$  materials should satisfy other requirements like wide band gap, large band offset to silicon for low leakage current, good thermodynamic stability, high interface quality, appropriate film morphology, good reliability, and process compatibility. Several materials such as Si<sub>3</sub>N<sub>4</sub>, Al<sub>2</sub>O<sub>3</sub>, Y<sub>2</sub>O<sub>3</sub>, La<sub>2</sub>O<sub>3</sub>, Pr<sub>2</sub>O<sub>3</sub>, HfO<sub>2</sub>, and ZrO<sub>2</sub> have been proposed from these viewpoints.<sup>1)</sup>

Among various methods which have been investigated to deposit these high- $k$  thin films on Si(100) surface, metal-organic chemical vapor deposition (MOCVD) is a leading deposition technique because of good surface coverage and large-area uniformity. In order to fabricate such ultra-thin films below ten nanometers with good reproducibility and good throughput by MOCVD, it is desirable to establish a reliable technique to monitor the deposition process and to control the film thickness and quality with an atomic-layer precision. Unlike electron beam methods that require ultra high vacuum, optical monitoring techniques are useful under low vacuum conditions routinely encountered during MOCVD processes. Specifically, spectroscopic ellipsometry is a promising technique for *in situ* monitoring of CVD growth of thin films.<sup>2)</sup> In this paper, the preparation of high- $k$  thin films by pulsed-source MOCVD, combined with *in situ* spectroscopic ellipsometry, is discussed.

### 2. Experimental

Among several materials, Y<sub>2</sub>O<sub>3</sub> has been chosen for the present study. Y<sub>2</sub>O<sub>3</sub> is an attractive candidate because of a rather large band gap ( $\sim 6$  eV), a high dielectric constant ( $k \sim 9 - 14$ ), and good chemical stability.<sup>3)</sup> P-type Si (100) wafers on which 1 nm nitride layer was prepared by direct nitridation at 800°C using NH<sub>3</sub>, were used as substrates to reduce the formation of SiO<sub>x</sub> at the interface between Si and yttrium oxide. A schematic diagram of the MOCVD growth chamber is shown in Fig. 1. O<sub>2</sub> gas was used as the

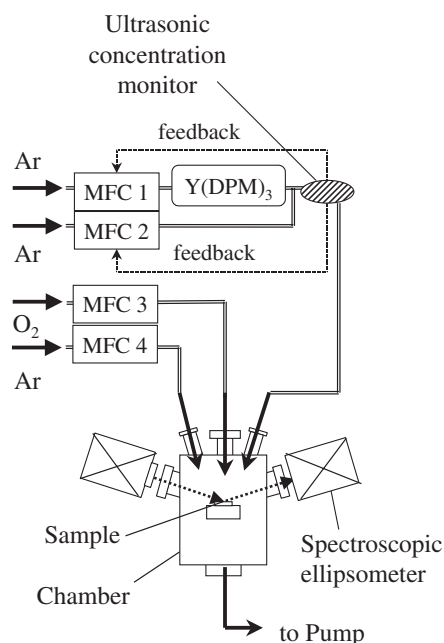


Fig. 1. A schematic diagram of the present MOCVD system. Air actuator valves to control the alternate supply of gas sources are introduced into the transfer line between the reaction chamber and vaporizers.

oxidizing agent.  $\beta$ -diketonate complex (Y(DPM)<sub>3</sub>) was used as the source for yttrium and was supplied to the chamber by Ar carrier gas. The temperature of the vaporizer was kept at a temperature of 140°C during operation. The gas transfer tubes were heated at a temperature of 180°C, higher than that of the vaporizer, to avoid the condensation of the precursor in the gas transfer tube. The pressure in the vaporizer was about 150 Torr. The concentration of Y(DPM)<sub>3</sub> was maintained with a feedback controlled system using ultrasonic sensor EPISON II (Thomas Swan Co. Ltd.). Details of the feedback system have already been published elsewhere.<sup>4)</sup> In our pulsed-source MOCVD method, yttrium compound and oxygen were supplied alternately. Ar purge gas was supplied between the alternating supply of gases. It was difficult to achieve an ideal self-limiting condition when  $\beta$ -diketon type precursor was used because of steric hindrance arising from the large size of the ligands.<sup>5)</sup> However, for obtaining thin films with atomic level precision, pulsed source MOCVD technique without self-limiting

\*E-mail address: tsuchi@diana.pe.titech.ac.jp

Table I. A list of deposition condition for each sample. Meaning of each parameter is described in the text.

| Name | $t_{\text{source}}$ (s) | $t_{\text{O}_2}$ (s) | $t_{\text{purge}}$ (s) | # of cycles | $T_s$ ( $^{\circ}\text{C}$ ) | CET (nm) | $J_g$ ( $\text{A}/\text{cm}^2$ ) |
|------|-------------------------|----------------------|------------------------|-------------|------------------------------|----------|----------------------------------|
| A    | 25                      | 30                   | 10                     | 62          | 500                          | —        | —                                |
| B    | 25                      | 15                   | 5                      | 120         | 600                          | —        | —                                |
| C    | 20                      | 20                   | 5                      | 10          | 560                          | —        | —                                |
| D    | 25                      | 60                   | 10                     | 58          | 500                          | 4.4      | $3.0 \times 10^{-5}$             |
| E    | 25                      | 15                   | 10                     | 71          | 500                          | —        | —                                |
| F    | 22                      | 15                   | 5                      | 16          | 560                          | 1.7      | $6.2 \times 10^{-3}$             |
| G    | 22                      | 20                   | 5                      | 16          | 560                          | 2.3      | $5.6 \times 10^{-4}$             |
| H    | 25                      | 60                   | 10                     | 52          | 600                          | 4.8      | $4.3 \times 10^{-7}$             |

mechanism still has advantages over conventional, uniform-flow, MOCVD.<sup>6)</sup> To hold the total pressure in the reaction chamber during deposition to 1.5 Torr, the flow rates of all gases were adjusted before the deposition. The supply durations of source-carrying Ar, O<sub>2</sub>, and the Ar purge gas in a cycle, here referred to as  $t_{\text{source}}$ ,  $t_{\text{O}_2}$ , and  $t_{\text{purge}}$ , respectively, were important parameters which were varied in these experiments. The substrate temperature ( $T_s$ ) was maintained at between 500 and 600 $^{\circ}\text{C}$  during deposition. From secondary ion mass spectrometry analysis, it was confirmed

that carbon impurities in the yttrium oxide layer, deposited at 560 $^{\circ}\text{C}$ , were the same level in the silicon substrates. Deposition conditions for samples used in this study are summarized in Table I.

*In situ* ellipsometry measurements were performed using a spectroscopic phase-modulated ellipsometer, UVISEL (Jobin-Yvon), which was installed on the reaction chamber as shown in Fig. 1. This equipment is capable of measuring the ellipsometric signal at a rate of 1 ms per single wavelength. Through the quartz window of the chamber, incident light was introduced at an angle of about 70 degrees from the substrate normal. Reflected light passed through another quartz window and was detected by an analyzer. Ar purge gas was introduced through the port near these two windows to avoid depositions on the quartz windows which may otherwise affect the ellipsometry signal.

### 3. Results and Discussions

First, we briefly describe the results of structural properties of deposited films. A cross-sectional transmitted electron microscope (TEM) image of a deposited film (sample A) is shown in Fig. 2. Polycrystalline films were obtained for all deposition temperatures used in this study. A 3nm-thick

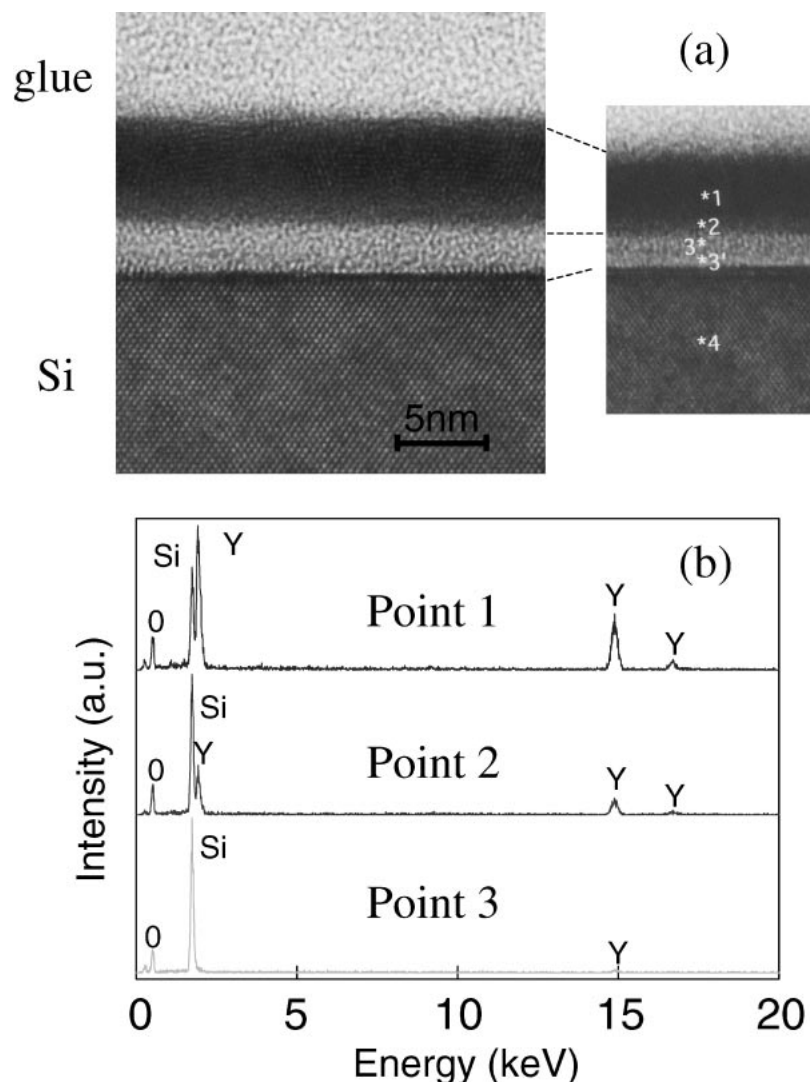


Fig. 2. (a) Cross-sectional HRTEM image of a yttrium oxide film (Sample A in Table I). The numbers shown in the right image indicate the point where the EDX analysis was performed. (b) EDX intensities at specific points in Sample A.

interfacial layer is clearly observed under the 6nm-thick yttrium oxide layer. On bare Si substrates without the silicon nitride layer, similar interfacial layers were also observed. This result shows that such a thin nitride layer on the Si wafer is not effective for preventing the formation of interfacial layer. High-resolution energy dispersive X-ray spectroscopy (EDX) measurement showed that yttrium was not detected in the interfacial layer region (point 3 in Fig. 2). Thus this interfacial layer was identified as SiO<sub>x</sub>. Si was detected not only at point 3 but also at point 2, where the concentration of Si was still larger than that of yttrium. It is indicative that even in the region with dark contrast in Fig. 2, there is a graded distribution of Si from the interface to the top of the film.

From ellipsometry angles,  $\Psi$ ,  $\Delta$ , which were directly measured by ellipsometry, we can calculate the pseudodielectric function  $\langle\epsilon(E)\rangle = \langle\epsilon_r\rangle + i\langle\epsilon_i\rangle$ .  $\langle\epsilon(E)\rangle$  is related to the optical constant of the materials which form the film, and the thickness of the film. To show typical time evolution of the real and the imaginary parts of the pseudodielectric function spectra,  $\langle\epsilon_r(E)\rangle, \langle\epsilon_i(E)\rangle$  during deposition of Y<sub>2</sub>O<sub>3</sub>, first we grew a film without alternate supply of gas sources at  $T_s = 600^\circ\text{C}$ . Spectra recorded at 5 minute intervals from the start of growth were shown in Fig. 3. A rapid change in the signal was observed during the initial 10 minutes of deposition. By fitting  $\langle\epsilon(E)\rangle$  with an appropriate model, additional information can be obtained, as discussed later. The measured thickness of the final oxide film (60 min, 24 nm) yields an average growth rate of about 0.4 nm/min. However, a film thickness of about 7 nm was estimated from the spectrum at 10 minutes into the growth. This higher

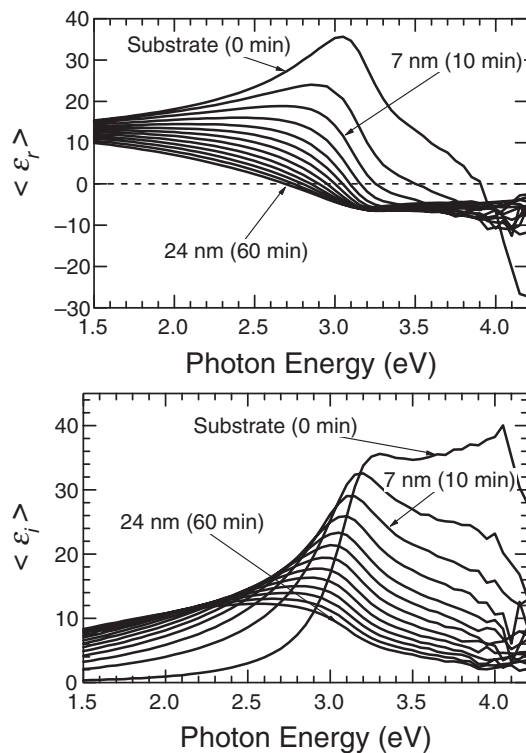


Fig. 3. Typical time evolution of  $\langle\epsilon_r\rangle$  and  $\langle\epsilon_i\rangle$  spectra obtained by ellipsometry measurement during deposition of Y<sub>2</sub>O<sub>3</sub> films. The film thickness shown in these figures were roughly estimated by fitting of each spectrum.

initial growth rate suggests that the rapid growth of the interfacial layer took place in the initial period on this growth condition.

For real-time monitoring of film growth, measurement at a specific wavelength has an advantage in terms of time resolution. We focus on the data of a selected photon energy, 4.1 eV. The time evolution of  $\langle\epsilon_r\rangle$  and  $\langle\epsilon_i\rangle$  of sample A is shown in Figure 4. Except for small oscillatory behavior, the value of  $\langle\epsilon_i\rangle$  displays a monotonically decrease with the growth of film, likely as a result of the increase in the film thickness. In fact, all films with growth terminated when  $\langle\epsilon_i\rangle$  reached a present value, *e.g.* the dashed line in Fig. 4, were found to have almost identical thicknesses. Monotonically decrease of  $\langle\epsilon_i\rangle$  with time suggested that the growth rate of the deposition with pulsed-source supply was more uniform through the growth than that without one, in which initial growth rate was higher as shown in Fig. 3. It is noted that the oscillating structure as clearly observed in the time dependence of  $\langle\epsilon_r\rangle$  and  $\langle\epsilon_i\rangle$ , had a period of oscillation which was matched to the cycle of gas supply. Therefore, changes of  $\langle\epsilon_r\rangle$  and  $\langle\epsilon_i\rangle$  within a cycle reflect a periodic change of the surface of the film due to the alternate supply of the gases. An average growth rate per one cycle is  $\sim 0.1$  nm, which can be compared to the thickness of a single molecular layer of Y<sub>2</sub>O<sub>3</sub>, 0.30 nm. From this observation, it is obvious that ellipsometry is an effective method for *in situ* monitoring of the fabrication of thin films with atomic layer-level sensitivity.

Next, we discuss the non-destructive determination of the layer structure of thin film by fitting the ellipsometry spectrum. For the fabrication of high-*k* thin films on the Si(001) surface, it is a general problem to avoid/control the formation of interfacial layer between the film and Si substrate. The non-destructive nature of the spectral analysis of ellipsometric signal can be taken advantage of to monitor possible interface reaction. When an appropriate model is assumed, various layer parameters, such as the thickness and the dielectric constant of each individual layer can be obtained by curve fitting. Under favorable conditions, the composition profile of a mixed film can be also modeled.<sup>7,8)</sup> Here we adopted a triple-layer model based on the results of analysis described earlier. In the middle layer, we use the effective-media approximation.<sup>7)</sup> Pseudodielectric function spectra of sample B with their fitting curves, and the layer structure determined by fitting are shown in Fig. 5, where  $\chi^2$  is the index of fitting. The small value of  $\chi^2 = 0.19$  indicates

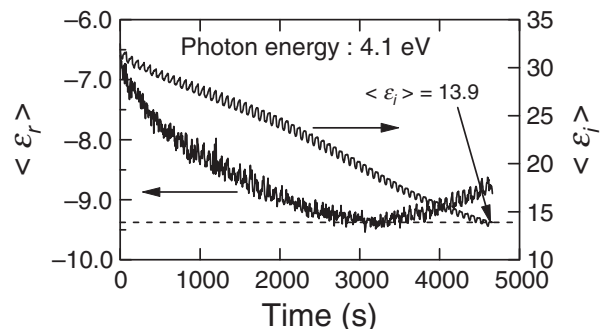


Fig. 4. Time evolution of  $\langle\epsilon_r\rangle$  and  $\langle\epsilon_i\rangle$  of sample A in Table I at 4.1 eV.  $\langle\epsilon_i\rangle$  value at the end of deposition is shown explicitly.

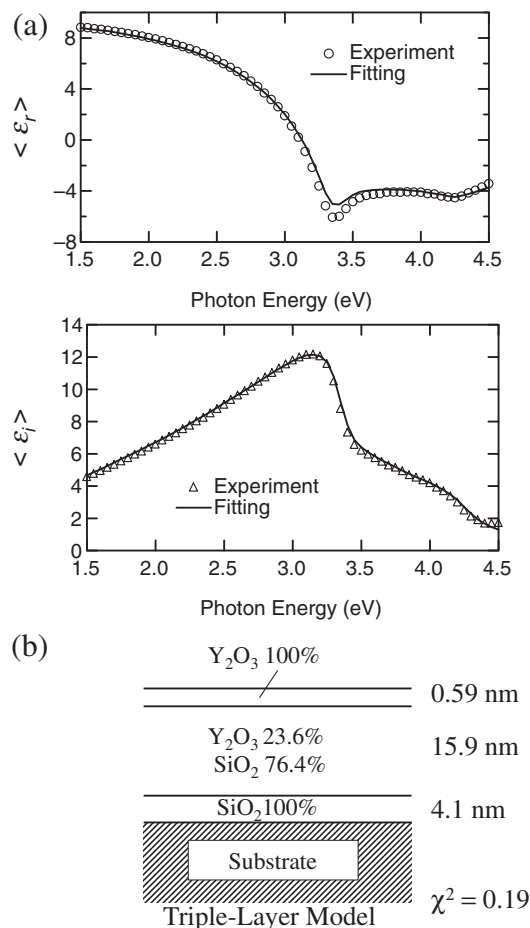


Fig. 5. (a) Fitting curve by using the triple-layer model is shown together with the experimental result of sample B in Table I. (b) Structural properties of sample B determined by the curve fitting are shown. Mean Squared Error,  $\chi^2$ , is also shown in this figure.

the high quality of the fit. The layer structure determined by ellipsometry is in qualitative agreement with the result of TEM-EDX observation. Although the spectra used in this analysis is that of the final layer, it might be possible to apply such spectral analysis *in situ* to investigate the formation of the interfacial layer during growth.

In the following, we compare ellipsometry results with results obtained by other physical methods. In Fig. 6(a), surface morphology data of sample C measured by atomic force microscopy (AFM) are shown. Note that the root mean square (RMS) of the sample in Fig. 6(a) is 0.26 nm, which is smaller than the thickness of a single molecular layer of  $\text{Y}_2\text{O}_3$ . Thin films with an average roughness smaller than the thickness of a single molecular layer were obtained. The correlation between the surface roughness and the ellipsometric signals has been discussed in the literature.<sup>7)</sup> The effect of surface roughness is often revealed in 2D  $\langle \epsilon_r \rangle - \langle \epsilon_i \rangle$  plots, with  $\langle \epsilon_r \rangle$  as the horizontal axis and  $\langle \epsilon_i \rangle$  as the vertical axis. Trajectories of ellipsometry signals of sample D and sample E, plotted in the  $\langle \epsilon_r \rangle - \langle \epsilon_i \rangle$  plane, together with the corresponding surface roughness data were shown in Fig. 6(b). These two samples were grown under identical conditions, with the exception that different oxygen supply durations,  $t_{\text{O}_2}$  were used. Insufficient oxidation of yttrium precursor caused by reduction of oxygen duration time might increase the average surface roughness, which was

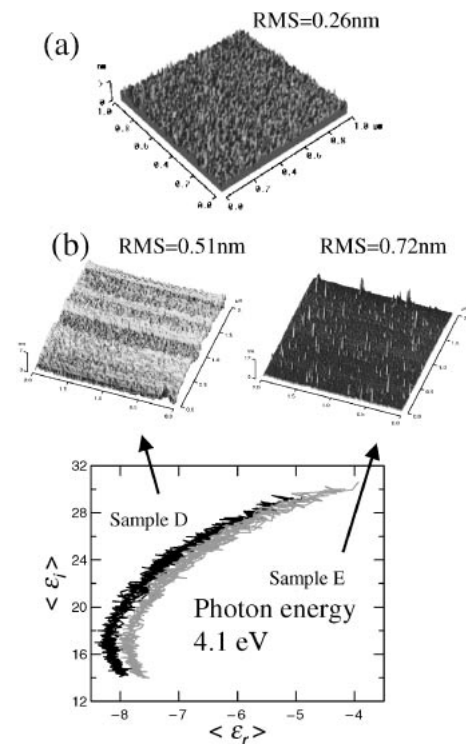


Fig. 6. (a) Surface roughness of sample C in Table I measured by AFM. (b) Trajectories of ellipsometry signal in  $\langle \epsilon_r \rangle - \langle \epsilon_i \rangle$  plane for two different samples (sample D and E in Table I). AFM images of each sample are also shown.

consistent with our results. A shift to larger  $\langle \epsilon_r \rangle$  is observed for the sample with larger surface roughness, as shown in Fig. 6, and this behavior is consistent with the overlayer theory.<sup>7)</sup> However, this shift is comparable to the noise level of  $\langle \epsilon_r \rangle$ . More careful measurements are needed to clarify the effect of surface morphology on the ellipsometric signal.

Electrical characteristics of Au/ $\text{Y}_2\text{O}_3$ /Si/Al structures fabricated in the present study were shown in Fig. 7. From the accumulation capacitance in a capacitance-voltage curve of the sample, we calculated the capacitance equivalent thickness (CET). The leakage current,  $J_g$ , was defined as the current density at  $-1$  V. Results of thinner films (sample F and G) are shown in Fig. 7(a) and (b). CET values as small as  $\sim 1.7$  nm have been obtained in sample F. However, films with smaller CET tend to have larger  $J_g$ . In Fig. 7(c) and (d), results of thicker ones are also shown. It can be seen, from Figs. 7(b) and 7(d), that films with longer oxygen exposure time (larger  $t_{\text{O}_2}$ ) and films deposited at higher temperature ( $600^\circ\text{C}$ ) tend to have smaller leakage currents. These results might be related to a difference in the thickness or the quality of its interfacial layer. CET and  $J_g$  of each sample are summarized in Table I. It is interesting to judge the dielectric properties of film from a ellipsometric signal during the growth. However, no obvious relationship between the electronic properties and the ellipsometry signal was found in the present study. More investigation is under way.

#### 4. Conclusion

We demonstrated that spectroscopic ellipsometry was an effective method for *in-situ* monitoring of the fabrication of



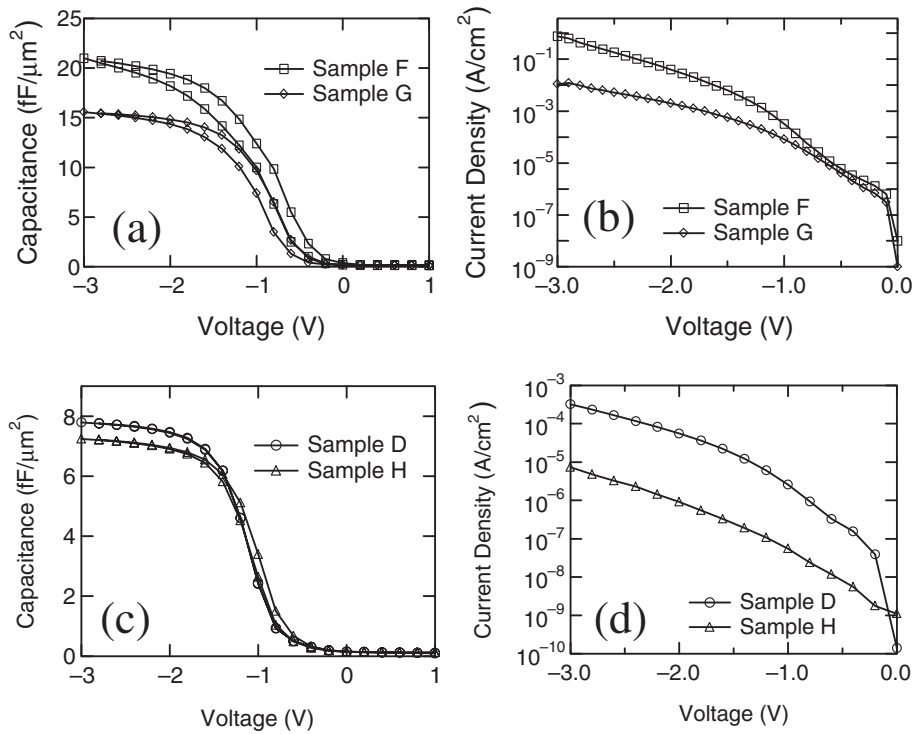


Fig. 7. Obtained electrical properties of Au/Y<sub>2</sub>O<sub>3</sub>/Si/Al structure are summarized. (a)  $C - V$  and (b)  $J - V$  in sample F and G, (c)  $C - V$  and (d)  $J - V$  in sample D and H. The deposition conditions of each sample is listed in Table I

high- $k$  dielectric thin films with the thickness of several nm by pulsed-source MOCVD. Thin yttrium oxide films with average roughnesses smaller than the thickness of a single molecular layer, and with CET  $\sim 1.7$  nm were obtained. Thicknesses and optical properties of each individual layer can also be extracted from spectroscopic ellipsometry, by fitting to appropriate structural models.

**Acknowledgements**

This work was partly supported by Grants-in-Aid for Scientific Research sponsored by the Japan Society for the Promotion of Science.

- 1) G. D. Wilk, R. M. Wallace and J. M. Anthony: J. Appl. Phys. **89** (2001) 5243.
- 2) S. Yamamoto, S. Sugai, Y. Matsukawa, A. Sengoku, H. Tobisaka, T. Hattori and S. Oda: Jpn. J. Appl. Phys. **38** (1999) L632.
- 3) M. Putkonen, T. Sajavaara, L.-S. Johansson and L. Niinisto: Chem. Vap. Deposit. **7** (2001) 44.
- 4) S. Yamamoto, K. Nagata, S. Sugai, A. Sengoku, Y. Matsukawa, T. Hattori and S. Oda: Jpn. J. Appl. Phys. **38** (1999) 4727.
- 5) S. Oda, H. Zama, K. Fujii, K. Sakai and Y. C. Chen: Thin Solid Films **225** (1993) 284.
- 6) S. Yamamoto and S. Oda: Chem. Vap. Deposit. **7** (2001) 7.
- 7) D. E. Aspnes, J. B. Theeten and F. Hottier: Phys. Rev. B **20** (1979) 3292.
- 8) P. J. McMarr, K. Vedam and J. Narayan: J. Appl. Phys. **59** (1986) 694.